

Supporting Information for:

Novel Pyrrolopyrimidine-Based α -Helix Mimetics: Cell-Permeable Inhibitors of Protein-Protein Interactions

Ji Hoon Lee,[†] Qi Zhang,[†] Sunhwan Jo,[‡] Sergio C. Chai,[†] Misook Oh,[†] Wonpil Im,[‡] Hua Lu,^{*†} and Hyun-Suk Lim^{*†}

Department of Biochemistry and Molecular Biology, and Indiana University Simon Cancer Center, Indiana University School of Medicine, Indianapolis, Indiana 46202 and Department of Molecular Biosciences and Center for Bioinformatics, The University of Kansas, 2030 Becker Drive, Lawrence, KS 66047

E-mail: limhyun@iupui.edu; hualu@iupui.edu

Table of Contents

1. Complete List of Authors for Reference 6
2. Complete List of Authors for Reference 11
3. Materials and General Methods
4. General Procedure for Synthesis
5. Library Synthesis
6. Resynthesis
7. Computational Structure Optimization, Docking, and Visualization
8. Plasmid Constructs and Protein Production
9. Fluorescence Polarization Assays
10. Cell Culture and Western Blot
11. Caspase Assays
12. References
13. Supporting Figures S1-S6
14. Table S1

Complete List of Authors for Reference 6:

Clark, M. P.; George, K. M.,; Bookland, R. G.; Chen, J.; Laughlin, S. K.; Thakur, K. D.; Lee, W.; Davis, J. R.; Cabrera, E. J.; Brugel, T. A.; VanRens, J. C.; Laufersweiler, M. J.; Maier, J. A.; Sabat, M. P.; Golebiowski, A.; Easwaran, V.; Webster, M. E.; De, B.; Zhang, G. *Bioorg. Med. Chem. Lett.* **2007**, *17*, 1250.

Complete List of Authors for Reference 11:

Laurie, N. A. Donovan, S. L.; Shih, C. S.; Zhang, J.; Mills, N.; Fuller, C.; Teunisse, A.; Lam, S.; Ramos, Y.; Mohan, A.; Johnson, D.; Wilson, M.; Rodriguez-Galindo, C.; Quarto, M. Francoz, S.; Mendrysa, S. M.; Guy, R. K.; Marine, J. C.; Jochemsen, A. G. Dyer, M. A. *Nature* **2006**, *444*, 61.

Materials and General Methods:

Unless otherwise noted, all chemicals and reagents were purchased from commercial suppliers (Sigma-Aldrich and Acros) and used without further purification. Rink amide MBHA resin (0.69 mmol/g) was purchased from Novabiochem. LC/MS characterization was performed on an Agilent 1200 LC/MS system (Agilent Technology) with a C18 reversed-phase column (Agilent Technology, 5 μ M, 4.6 mm x 125 mm). A gradient elution of 100% A in 4 min followed by 90% B in 20 min was used at flow rate of 1 mL/min (solvent A: H₂O, 0.1% TFA; B: acetonitrile, 0.1% TFA). Preparative HPLC purification was performed on an Agilent 1120 Compact LC system (Agilent Technology) with a C18 reversed-phase column (Agilent Technology, 5 μ M, 25 mm x 125 mm) using a linear gradient from 10% B to 100% B by changing solvent composition over 40 minutes. Peptoid synthesis under microwave conditions was performed in a 1000 W Whirlpool microwave oven (model MT4155SPT) with 10% power. Thermal reactions were carried out in a heating mantle filled with sea sand using 4 ml glass vials (Fisher Scientific).

General Procedure for Synthesis:

Rink amide MBHA resin (100 mg, 56 μmol) was swelled with dimethylformamide (DMF) (2 mL) in a 5 mL fritted syringe for 2 h. The Fmoc protecting group on the resin was removed by treating with 20 % piperidine in DMF (2 x 10 min). To the resin, two peptoid residues were added by a standard submonomer route [1] using a microwave-assisted protocol [2]. At the end of the reaction, the reaction mixture was drained and the resins were washed with DMF (3 \times), CH_2Cl_2 (2 \times), MeOH (2 \times), and DMF (3 \times). The resin was treated with 4,6-dichloro-2-methylthio-5-formylaldehyde (5 equiv.) and triethylamine (TEA) (5 equiv.) in tetrahydrofuran (THF) at room temperature overnight. The reaction mixture was drained and washed with DMF (3 \times), CH_2Cl_2 (2 \times), MeOH (2 \times), and DMF (3 \times). For cyclization and dimethylamination, the resins were reacted with 1,8-diazabicyclo[5.4.0]undec-7-ene (DBU) (20 equiv.) in DMF (2 mL) and MeOH (1 mL) at 90 $^\circ\text{C}$ overnight. After thorough washing, the sulfide group was oxidized into a sulfone by treating with m-chloroperoxybenzoic acid (mCPBA) (10 equiv.) and NaHCO_3 (15 equiv.) in THF (2 mL)/ H_2O (400 μL) at room temperature overnight. The resin was thoroughly washed with DMF (3 \times), CH_2Cl_2 (2 \times), MeOH (2 \times), and DMF (3 \times). The resulting sulfone group was replaced with various amines (Figure S2) by treating with an amine (20 equiv.) and N,N-diisopropylethylamine (DIEA) (100 equiv.) in N-methyl-2-pyrrolidone (NMP) at 170 $^\circ\text{C}$ overnight. After thorough washing with DMF (3 \times), CH_2Cl_2 (2 \times), MeOH (2 \times), and CH_2Cl_2 (5 \times), the products were cleaved from the resin using a cleavage cocktail (95% trifluoroacetic acid (TFA), 2.5% triisopropylsilane, and 2.5% water) for 2 h at room temperature.

Library Synthesis:

A library of compound **3** was synthesized manually in a parallel fashion. After Fmoc deprotection, NH_2 group of Rink amide MBHA resin (5 g) was bromoacetylated in a 250mL peptide synthesis vessel (Chemglass Life Sciences) to provide compound **4** (Scheme 1). After thorough washing, the resin was split into 10 fritted syringe reactors in equal quantities (\approx 500 mg of resin in each reactor).

The resin in each reactor was then treated with 10 different primary amines shown in Figure S2 to introduce R₁ group (giving 10 different monomeric peptoids **5** in Scheme 1). The peptoids **5** in 10 individual reactors were bromoacetylated, respectively. After that, the beads in each reactor were split into 9 reactors to couple with 9 different primary amines (R₂) shown in Figure S2. As a result, 90 different dimeric peptoids **6** were obtained (\approx 55 mg of resin in each reactor). After thorough washing, dimeric peptoids **6** in each reactor were transformed into sulfone compounds **9** by three steps, following the aforementioned procedure (Scheme 1). The resin was split into 10 reaction vials in equal quantities (\approx 5 mg of resin in each reactor). The 900 sulfone compounds in each reactor were then coupled with desired amines shown in Figure S2 to provide final products **3**. After cleavage with a cleavage cocktail (95% TFA, 2.5% triisopropylsilane, and 2.5% water), the crude product were dried by evaporating with a stream of nitrogen and dissolved in DMSO to make a \approx 10 mM stock solution.

Resynthesis:

Compounds **3a**, **3b**, and NC-1 were resynthesized on 100 mg of MBHA resin, following the general procedure as described above. After cleavage reaction, the crude compounds were purified by HPLC (Figure S5). The overall isolated yields of **3a**, **3b**, and NC-1 were 26%, 40%, and 42%, respectively.

Computational Structure Optimization, Docking, and Visualization:

The geometry-optimized structure of compound **3** (Figure 1C) was obtained as follows. First, its initial conformations were generated by the molecular mechanics simulation software CHARMM [3] with force field parameters obtained by Antechamber [4] using the AM1-BCC charge models and general AMBER force field [5]. The generated conformations were grouped into two conformations based on the structural similarity. We have chosen a representative conformation which has functional groups facing the same direction, and was subjected to geometry optimization at the HF/6-

31G* level using Gaussian 03 software [6]. We used the molecular visualization software PyMol [7] for Figures 1C, 2A, 2B, and Figure S3. In Figure 2A, MDMX is visualized with its molecular surface with surface charge distribution: red for negatively-charged residues and blue for positively-charged residues. Since the p53-MDMX complex (PDB entry: 2Z5S) is already known, instead of performing *de novo* docking of compound **3** onto MDMX, we performed the rigid-body fitting of the geometry-optimized structure of compound **3** to maximize the overlap between the functional groups of compound **3** and the side chains of the functionally important residues (F19, W23, and L26) in the p53 peptide using PyMol [7]. These overlaid structures are shown in Figure 2B and Figure S3.

Plasmid Constructs and Protein Production:

The gene encoding p53-binding domain of human MDMX (a.a. 1-137) or human MDM2 (a.a. 1-138) was amplified by polymerase chain reaction (PCR) and cloned into the pGEX-4T1 plasmid. The recombinant GST fusion proteins were expressed in BL21 (DE3) *E. coli* cells and purified by a 5-ml GSTrap HP column (GE Life Sciences) according to the manufacturer's instructions. Purified GST-tagged MDMX protein was used in the compound primary screening. For the dose-dependent assays, the GST-tags of MDMX and MDM2 were cleaved by thrombin, and purified through benzamidine FF and GSTrap HP columns. Proteins were concentrated by ultrafiltration (Millipore-Amicon ultra) and dialyzed against phosphate buffered saline (PBS) (pH 7.5) containing 2 mM phenylmethanesulfonylfluoride (PMSF), 10% glycerol and 1mM dithiothreitol (DTT).

Fluorescence Polarization Assays:

We adapted previously established fluorescence polarization (FP) assays [8,9] to monitor the displacement of a Rhodamine-labeled p53 peptide (Rd-p53 peptide) from MDMX or MDM2 by inhibitors or unlabeled p53 peptide (Figure S4A). The p53 peptide (SQETFSDLWKLLPEN-NH₂) and N-terminally labeled Rhodamine p53 peptide (SQETFSDLWKLLPEN-NH-Rhodamine) were

synthesized by the Antagene Inc. The p53 peptide binds to MDMX with $K_D \approx 0.9 \mu\text{M}$ and to MDM2 with $K_D \approx 0.4 \mu\text{M}$ (Figure S4B). K_D values were calculated as described previously [10]. The specificity of this assay was confirmed by the competitive displacement of the unlabeled p53 peptide and the specific MDM2 inhibitor MI-63 [11] using assay conditions as described below (Figure S4C). All FP assays were performed in 384-well black plates (Nalge Nunc International). For liquid transfer, Precision Microplate Pipetting System (BioTek Instruments, Inc.) was used.

For inhibition studies, in each well of the microtiter plates, 40 μl solution containing 1.5 μM of MDM2 or MDMX and 75 nM of the Rd-p53 peptide in 1 \times PBS (pH 7.5) with 0.01% Triton was combined with 20 μl of each library compound (final concentration of 40 μM and 2% DMSO). Following incubation at 23 $^\circ\text{C}$ for 30 min, the fluorescence signals (excitation at 531 nm and emission at 595 nm) were monitored using a SpectraMax M5^e (Molecular Devices). Positive controls (100% inhibition) contained Rd-p53 peptide only, and negative controls contained Rd-p53 peptide and MDMX or MDM2 proteins. The Z' factor, indicating the quality of a FP assay, was calculated based on the following equation: $Z' \text{ factor} = 1 - \frac{3 \times (SD_+ + SD_-)}{|\mu_+ - \mu_-|}$, where μ_+ and μ_- represent the means of the positive and negative control signals, respectively, and SD_+ and SD_- are standard deviations of the mean values for the positive and negative controls, respectively [12]. The FP assay achieved a Z' -factor of 0.8, based on negative (containing Rd-p53 peptide with MDMX or MDM2 proteins) and positive (containing Rd-p53 peptide only) controls (16 data points per positive and negative controls). The primary screen of a 900-compound library yielded 7 putative hits that inhibited the p53-MDMX by at least 50% (Figure S4D). By subsequent dose-dependent experiments of these compounds, two compounds, denoted **3a** and **3b**, were chosen for further studies. Inhibitory activity was calculated as the mean value of negative controls minus the average sample value divided by the mean value of negative controls minus the mean value of positive controls, multiplied by 100. Dose-dependent experiments were carried out using the same conditions as above. IC_{50}

values were determined by the Hill equation using Igor4.01 (Lake Oswego, Oregon, USA). *K_i* values were calculated by a web-based computer program developed for FP-based binding assays (http://sw16.im.med.umich.edu/software/calc_ki/) [13]. The primary screen experiments were performed in duplicate and the dose response experiments were performed in triplicate.

Cell Culture and Western Blot:

H460 cells were seeded in 6-well plates and grown in Dulbecco's modified Eagle's medium supplemented with 10% fetal bovine serum (FBS), 100 U per mL penicillin, and 100 U per mL streptomycin. Compounds **3a**, **3b**, and NC-1 were dissolved in DMSO and diluted directly into the medium to the indicated concentrations; 0.1% DMSO was used as a control. After incubation with the compounds for 12 h, cells were harvested and lysed in 50 mM Tris-HCl pH 8.0, 150 mM NaCl, 5 mM EDTA, 0.5% NP-40 supplemented with 2 mM DTT and 1 mM PMSF. An equal amount of protein samples (50 µg) was subjected to SDS-PAGE and transferred to a PVDF membrane (PALL Life Science). The membranes with transferred proteins were blocked with 1×TBST containing 5% non-fat, dried milk for 1h at room temperature, and then incubated with anti-p53 (mouse monoclonal, DO-1, Santa Cruz), anti-p21 (rabbit polyclonal, M19, Santa Cruz), or anti-β-actin antibodies (Sigma) followed by a secondary antibody labeled with horseradish peroxidase (Pierce). The blots were developed by an enhanced chemiluminescence detection kit (Thermo Scientific), and signals were visualized by Omega 12iC Molecular Image System (UltraLUM).

Caspase Assays:

H460 and H1299 cells were plated at 4×10^3 cells/well in white-walled 96-well plates, cultured for 24 h in DMEM with 10% FBS, and treated with **3a** (20 µM), NC-1 (20 µM), MI-63 (20 µM), and DMSO for another 24 h. The caspase 3/7 activity was measured using Caspase-Glo 3/7 Assay kit (Promega) according to the manufacturer's instructions. Briefly, 100 µl of caspase-Glo substrate reagent was added into each well containing 100 µl cell culture media and luciferase activity was

determined at room temperature using FlexStation II³⁸⁴ (Molecular devices) after 40 min.

References:

1. Figliozzi, G. M.; Goldsmith, R.; Ng, S. C.; Banville, S.C.; Zuckermann, R. N. *Methods Enzymol.* **1996**, *267*, 437.
2. Olivos, H. J.; Alluri, P. G.; Reddy, M. M.; Salony, D.; Kodadek, T. *Org. Lett.* **2002**, *4*, 4057.
3. Frisch, M. J. et al. Gaussian, Inc: Pittsburgh, PA, 2003.
4. Brooks, B. R.; Brooks, C. L. 3rd.; Mackerell, A. D. Jr.; Nilsson, L.; Petrella, R. J.; Roux, B.; Won, Y.; Archontis, G.; Bartels, C.; Boresch, S.; Caflisch, A.; Caves, L.; Cui, Q.; Dinner, A. R.; Feig, M.; Fischer, S.; Gao, J.; Hodoseck, M.; Im, W.; Kuczera, K.; Lazaridis, T.; Ma, J.; Ovchinnikov, V.; Paci, E.; Pastor, R. W.; Post, C. B.; Pu, J. Z.; Schaefer, M.; Tidor, B.; Venable, R. M.; Woodcock, H. L.; Wu, X.; Yang, W.; York, D. M.; Karplus, M. *J. Comput. Chem.* **2009**, *30*, 1545.
5. Wang, J.; Wang, W.; Kollman P. A.; Case, D. A. *J. Mol. Graph. Model.* **2006**, *25*, 247260.
6. Wang, J.; Wolf, R. M.; Caldwell, J. W.; Kollman, P. A.; Case, D. A. *J. Comput. Chem.* **2004**, *25*, 1157.
7. DeLano, W. L. 2002. The PyMOL Molecular Graphics System. Palo Alto, CA, USA.
8. Ding, K.; Lu, Y.; Nikolovska-Coleska, Z.; Qiu, S.; Ding, Y.; Gao, W.; Stuckey, J.; Krajewski, K.; Roller, P. P.; Tomita, Y.; Parrish, D. A.; Deschamps, J. R.; Wang, S. *J. Am. Chem. Soc.* **2005**, *127*, 10130.
9. Reed, D.; Shen, Y.; Shelat, A. A.; Arnold, L. A.; Ferreira, A. M.; Zhu, F.; Mills, N.; Smithson, D. C.; Regni, C. A.; Bashford, D.; Cicero, S. A.; Schulman, B. A.; Jochemsen, A. G.; Guy, R. K.; Dyer, M. A. *J. Biol. Chem.* **2010**, *285*, 10786.
10. Chai, S. C.; Ye, Q. Z. *BMC. Biochem.* **2009**, *10*, 32.
11. Shangary, S.; Qin, D.; McEachern, D.; Liu, M.; Miller, R. S.; Qiu, S.; Nikolovska-Coleska, Z.; Ding, K.; Wang, G.; Chen, J.; Bernard, D.; Zhang, J.; Lu, Y.; Gu, Q.; Shah, R. B.; Pienta, K. J.; Ling, X.; Kang, S.; Guo, M.; Sun, Y.; Yang, D.; Wang, S. *Proc. Natl. Acad. Sci. USA.* **2008**, *105*, 3933.
12. Arai, T.; Yatabe, M.; Furui, M.; Akatsuka, H.; Uehata, M.; Kamiyama, T. *Anal. Biochem.* In press.
13. Ding, K.; Lu, Y.; Nikolovska-Coleska, Z.; Wang, G.; Qiu, S.; Shangary, S.; Gao, W.; Qin, D.; Stuckey, J.; Krajewski, K.; Roller, P. P.; Wang, S. *J. Med. Chem.* **2006**, *49*, 3432.

Figure S1. LC/MS data of crude mixtures of representative intermediates and final products.

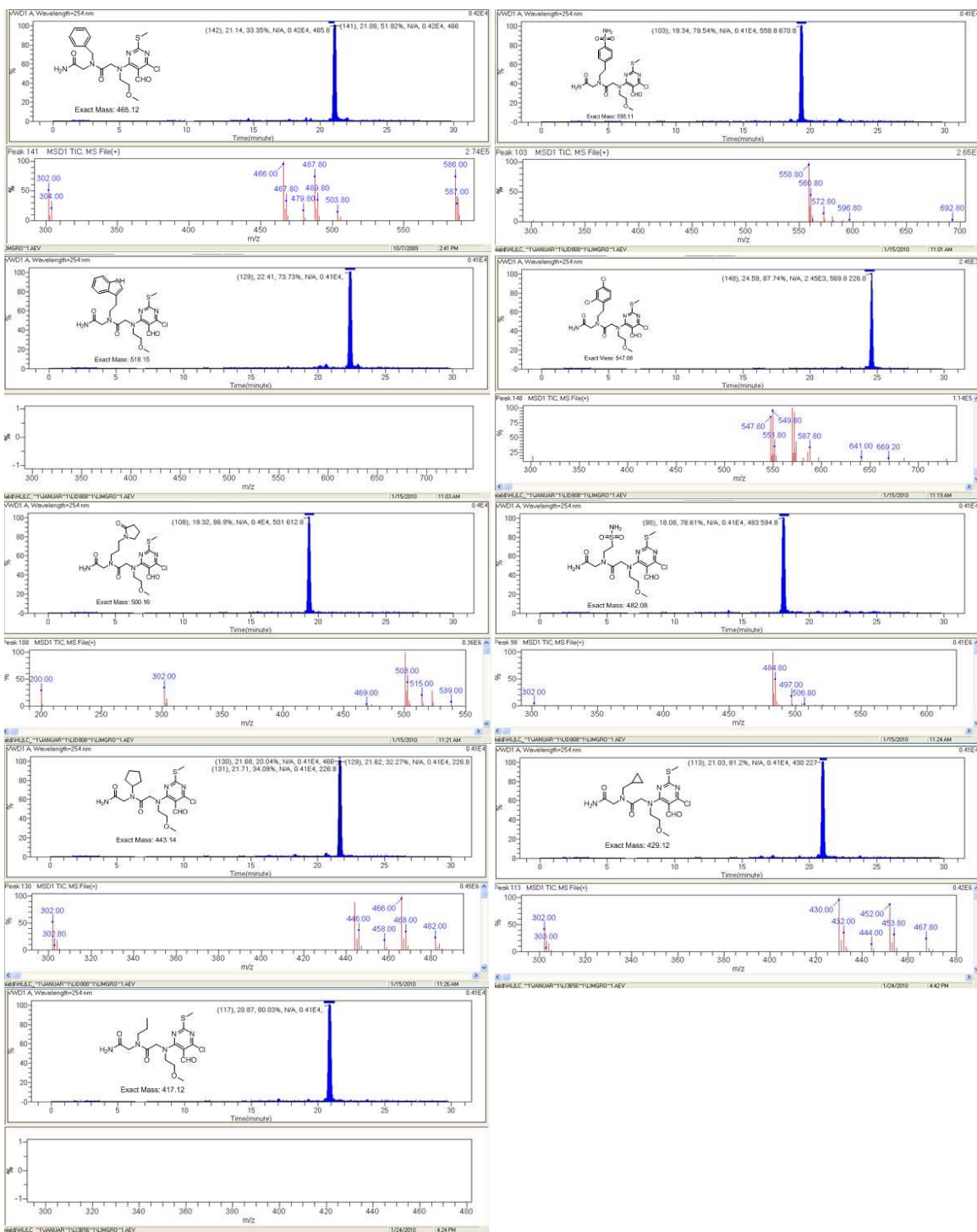
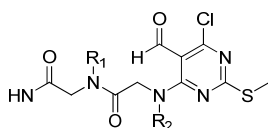


Figure S1. (Cont'd).

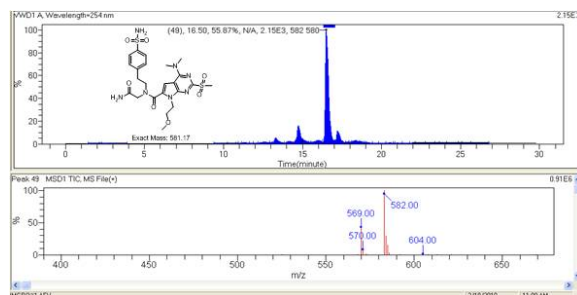
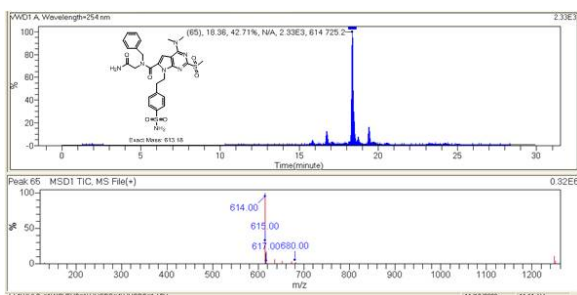
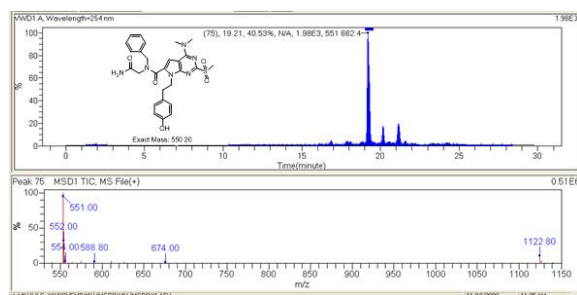
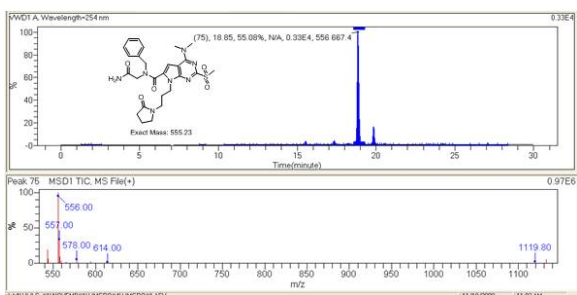
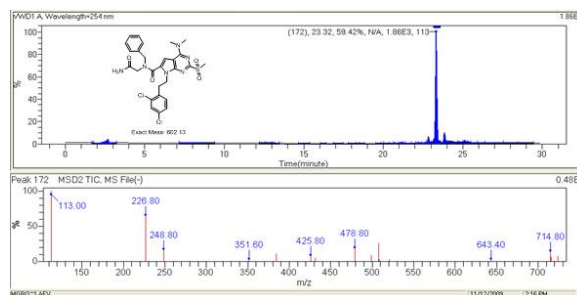
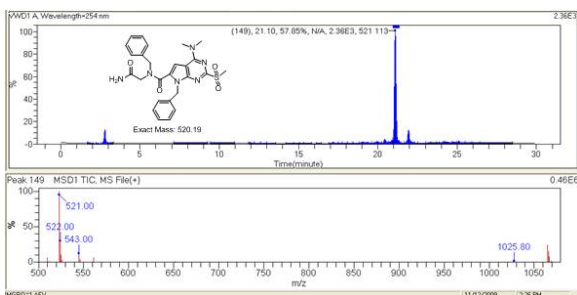
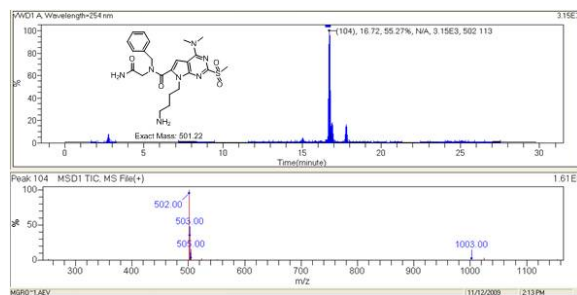
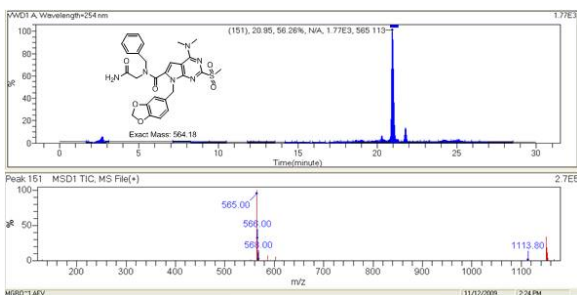
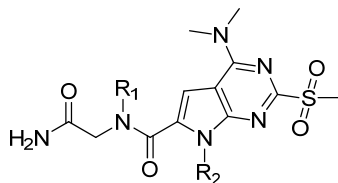


Figure S1. (Cont'd).

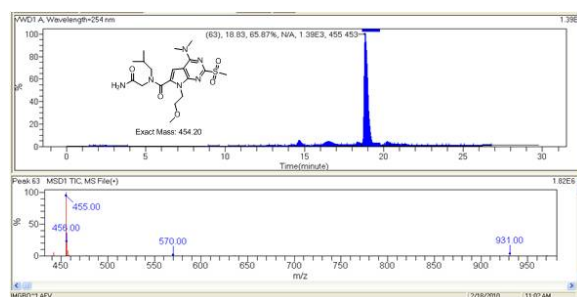
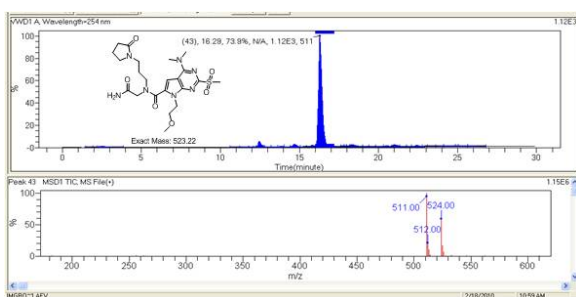
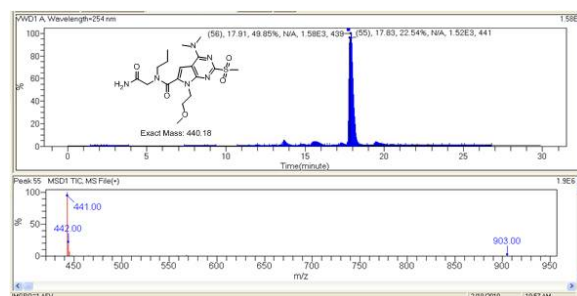
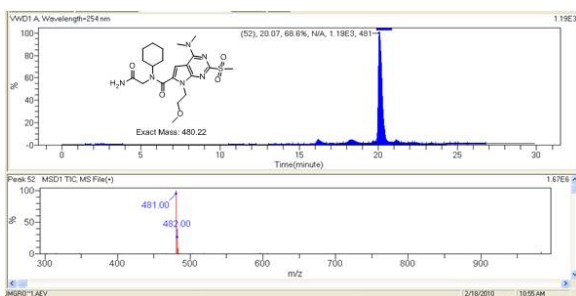
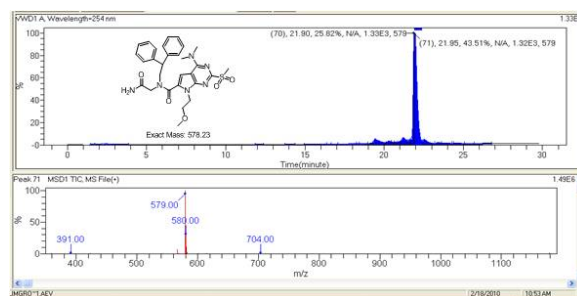
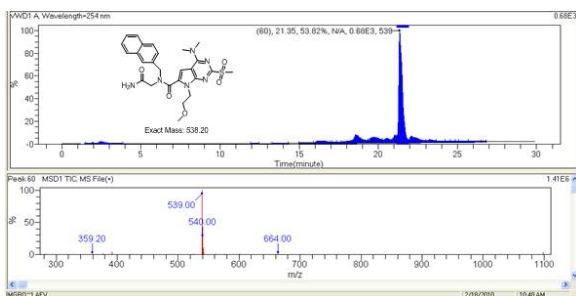
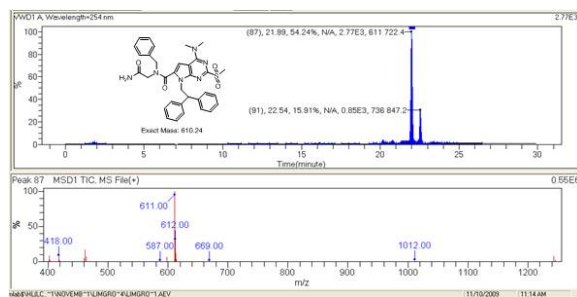
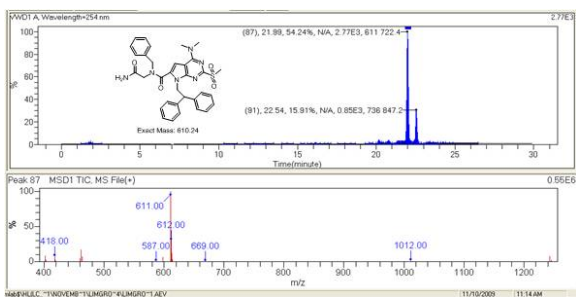


Figure S1. (Cont'd).

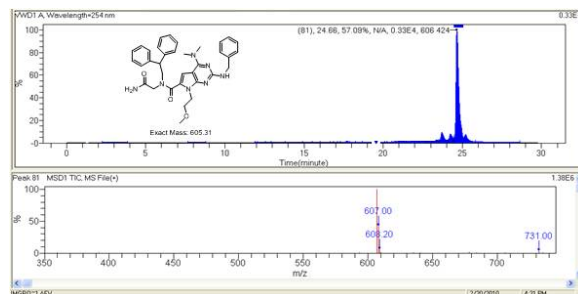
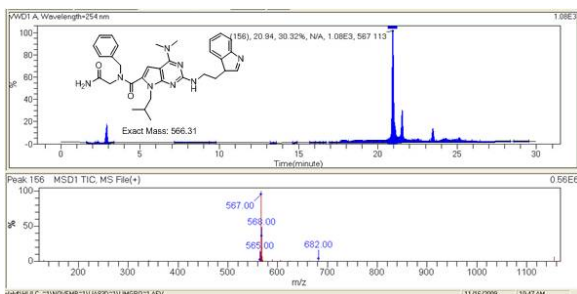
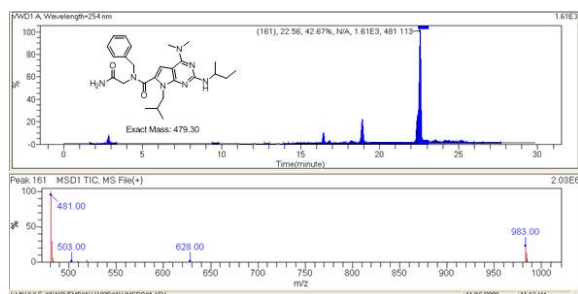
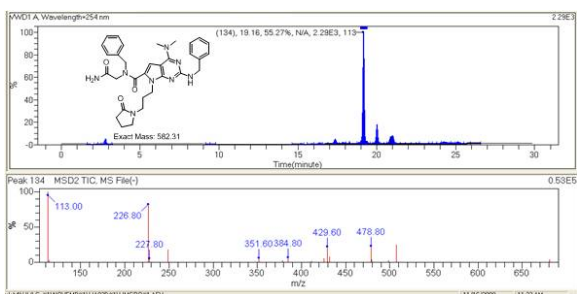
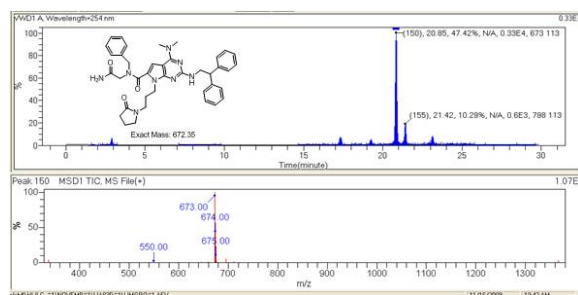
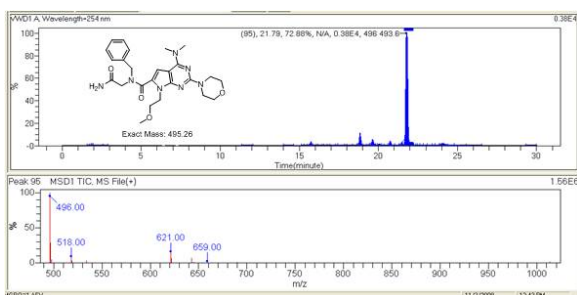
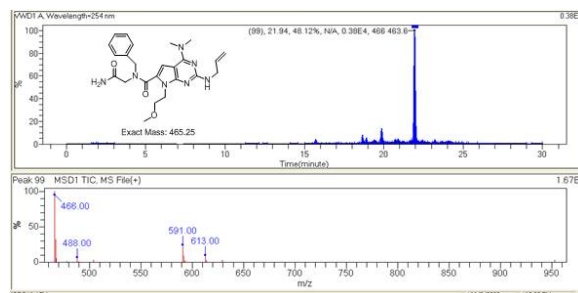
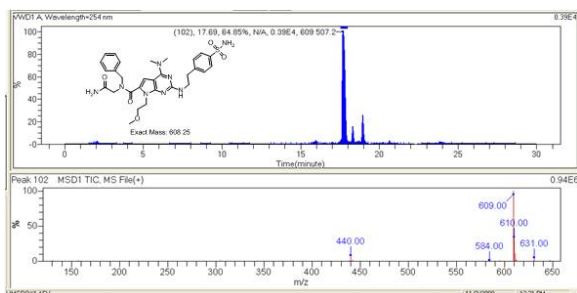
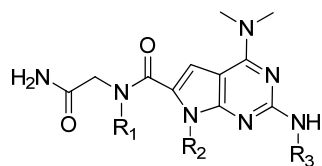


Figure S1. (Cont'd).

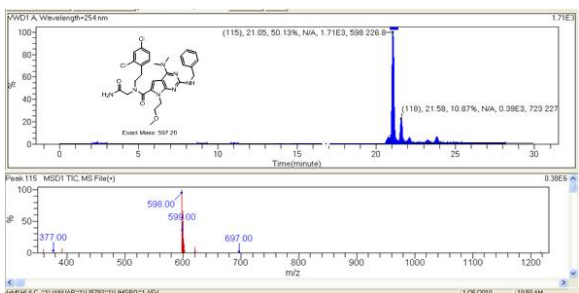
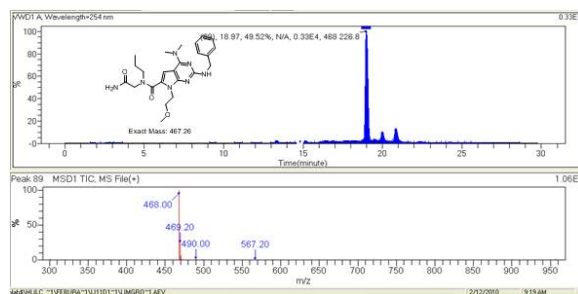
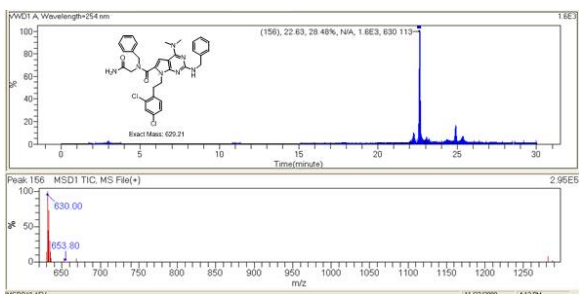
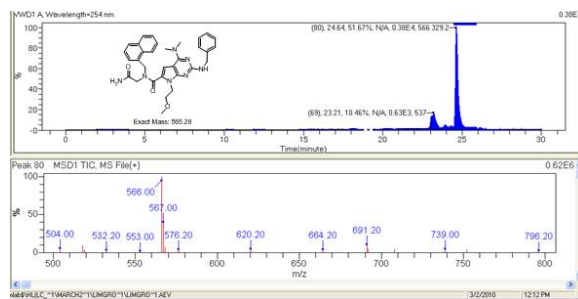
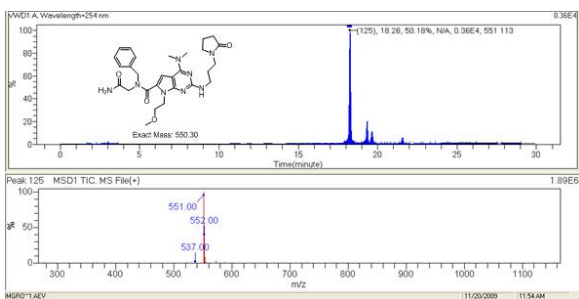
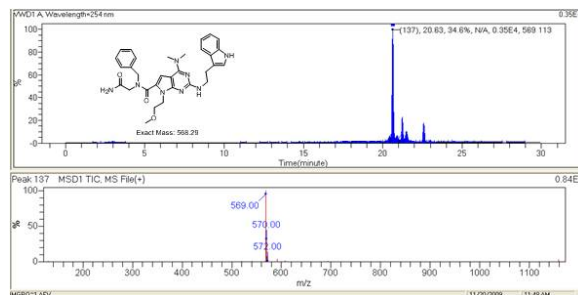
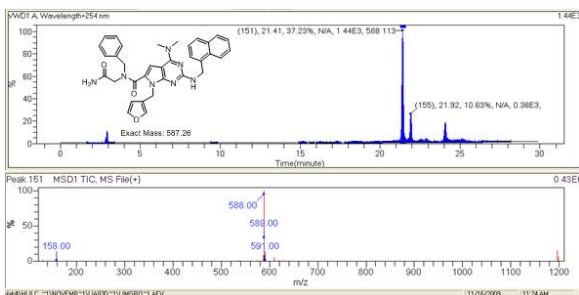


Figure S2. Amines used for the library synthesis.

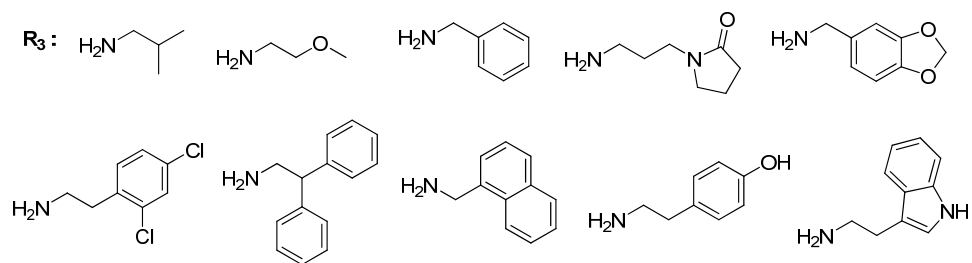
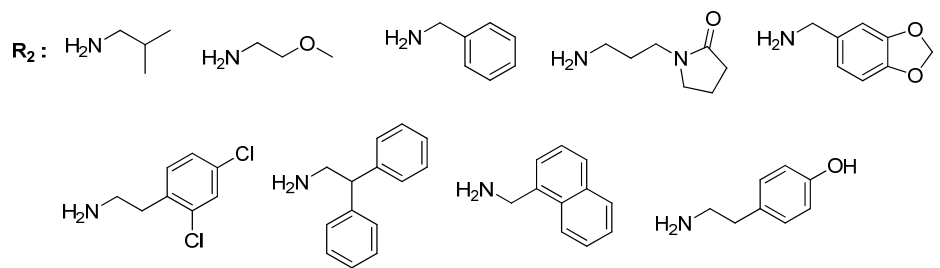
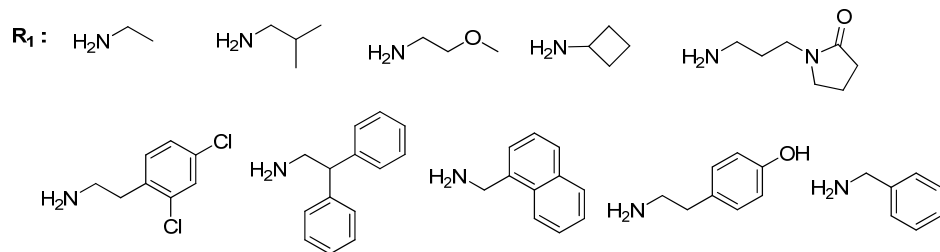
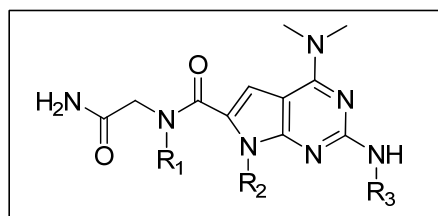
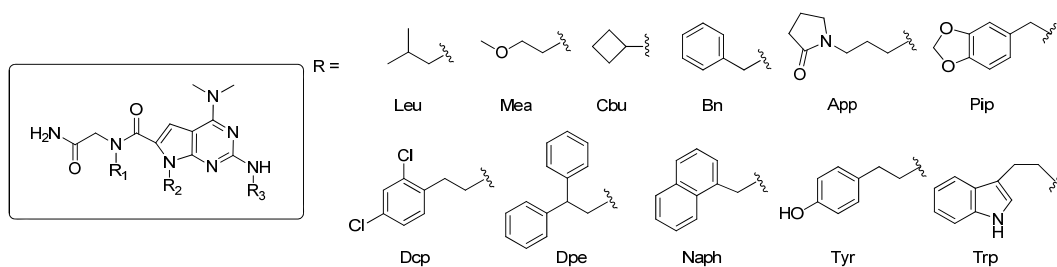


Table S1. Purity of the 90 compounds selected randomly from the 900-member library.



Entry	R ₁	R ₂	R ₃	Purity (%)	Calculated Mass (M)	Found Mass (M+H)
1	Dcp	Naph	Leu	89.6	645.24	646.00
2	Dcp	Dpe	Mea	89.4	687.25	688.00
3	Naph	Dcp	Bn	81.9	679.23	680.00
4	Mea	Bn	App	84.4	550.30	551.20
5	Leu	Mea	Dcp	70.4	563.22	564.20
6	Pip	Leu	Dpe	62.1	647.32	648.20
7	Bn	Pip	Naph	67.5	641.26	642.00
8	App	Bn	Tyr	92.9	612.32	613.00
9	Leu	Bn	Trp	70.2	566.31	567.20
10	Leu	Bn	Leu	82.6	479.30	480.20
11	Tyr	Leu	Mea	89.0	511.29	512.20
12	Dpe	Bn	Bn	87.2	637.32	638.20
13	Mea	Bn	App	89.5	550.30	551.20
14	Dcp	Dpe	Pip	64.9	763.24	764.00
15	Mea	Mea	Dcp	90.4	565.20	566.00
16	Leu	Bn	Dpe	74.5	603.33	604.20
17	Naph	Dcp	Naph	74.0	729.24	730.00
18	Dpe	Dpe	Tyr	92.2	757.38	758.00
19	Bn	Tyr	Trp	80.4	630.30	631.00
20	Naph	Bn	Leu	86.2	563.30	564.00
21	Bn	Dcp	Mea	96.0	597.19	598.00
22	App	Pip	Bn	82.6	626.30	627.00
23	App	Dcp	App	96.6	699.28	700.00
24	Dcp	Cbu	Dcp	91.0	675.13	676.00
25	Bn	Pip	Dpe	88.4	681.30	682.00
26	App	Pip	Naph	68.7	676.31	677.00
27	Tyr	App	Tyr	93.1	642.33	643.20
28	Mea	Bn	Trp	88.6	568.29	569.20
29	Dcp	App	Leu	81.0	630.26	631.00
30	Mea	Naph	Mea	94.3	533.28	534.00

Table S1. (Cont'd).

Entry	R₁	R₂	R₃	Purity (%)	Calculated Mass (M)	Found Mass (M+H)
31	Dcp	Leu	Bn	79.8	595.23	596.00
32	Cbu	Tyr	App	81.8	576.31	577.00
33	Dcp	Dcp	Dcp	86.1	793.08	793.80
34	Naph	Leu	Dpe	64.8	653.34	654.00
35	Bn	App	Naph	83.3	632.32	633.20
36	Dcp	App	Tyr	87.6	694.25	695.00
37	App	Mea	Leu	84.8	516.32	517.20
38	Mea	Naph	Mea	94.1	533.28	534.20
39	Leu	Leu	Bn	88.6	479.31	480.00
40	Dpe	Dpe	App	77.8	762.40	763.20
41	Naph	Naph	Dcp	89.9	729.24	730.00
42	Leu	Dcp	Dpe	67.6	685.27	686.00
43	Naph	App	Tyr	80.5	662.34	663.00
44	Dcp	Pip	Trp	66.7	726.22	727.00
45	App	Bn	Leu	82.9	548.32	549.00
46	Dpe	Tyr	Mea	83.4	635.32	636.00
47	Bn	Naph	Bn	86.8	597.29	598.00
48	Dpe	Pip	App	76.6	716.33	717.20
49	Naph	Dcp	Dcp	91.2	761.16	762.00
50	Cbu	Bn	Dpe	81.6	601.31	602.00
51	Bn	App	Naph	81.6	632.32	633.00
52	Dpe	Tyr	Tyr	93.7	697.34	698.00
53	Dpe	Mea	Trp	89.9	658.34	659.00
54	Naph	Tyr	Leu	88.4	593.31	594.20
55	App	Tyr	Mea	91.1	580.31	581.00
56	Leu	Naph	Bn	80.5	563.31	564.20
57	Dpe	Bn	App	83.1	632.32	673.20
58	Leu	Naph	Dcp	74.2	645.24	646.00
59	Dpe	Mea	Dpe	75.1	695.36	696.00
60	Bn	Naph	Tyr	85.6	627.30	628.00

Table S1. (Cont'd).

Entry	R₁	R₂	R₃	Purity (%)	Calculated Mass (M)	Found Mass (M+H)
61	Leu	Leu	Leu	80.5	445.32	446.00
62	Dpe	App	Mea	93.3	640.35	641.20
63	Pip	Naph	Bn	88.8	641.28	642.00
64	Tyr	Bn	App	84.1	612.31	613.20
65	Tyr	Cbu	Dcp	82.3	623.21	624.00
66	Naph	Dpe	Dpe	75.2	777.38	778.00
67	Dpe	Bn	Naph	70.7	687.33	688.20
68	Cbu	Pip	Tyr	92.9	585.26	586.00
69	Naph	Pip	Leu	88.7	607.29	608.00
70	Tyr	Tyr	Mea	87.9	575.28	576.00
71	Pip	Dcp	Bn	87.9	673.20	674.00
72	Tyr	Naph	App	67.3	662.33	663.00
73	Bn	Dpe	Dcp	69.1	719.25	720.00
74	Naph	Bn	Dpe	89.2	687.33	688.00
75	Bn	Naph	Tyr	85.5	627.30	628.00
76	Dpe	Bn	Trp	75.0	690.34	691.20
77	Dpe	Naph	Leu	83.4	653.35	654.20
78	Mea	Mea	Mea	94.1	451.26	452.20
79	Naph	Dcp	Bn	84.7	679.22	680.00
80	Leu	Bn	App	87.2	548.32	549.20
81	Mea	Bn	Tyr	88.9	545.28	546.00
82	Bn	Naph	Trp	88.2	650.31	651.00
83	Dcp	Naph	Leu	85.9	645.24	646.00
84	Cbu	Mea	Mea	92.8	447.25	448.00
85	Leu	Bn	Bn	69.3	513.29	514.20
86	Dpe	Dcp	App	68.3	754.29	755.00
87	Bn	Dpe	Dcp	86.7	719.25	720.00
88	App	Leu	Dpe	68.2	638.37	639.20
89	Dcp	Naph	Naph	75.5	729.24	730.00
90	Dpe	App	Tyr	93.6	702.37	703.00

Figure S3. (A) Co-crystal structure of the MDMX bound with a 12-mer p53 peptide. (B) A computational docking model of the MDMX in complex with compound **3** (a trimethyl-substituted form). (C) An overlay of a 12-mer p53 peptide and compound **3** on the p53 binding pocket in the MDMX.

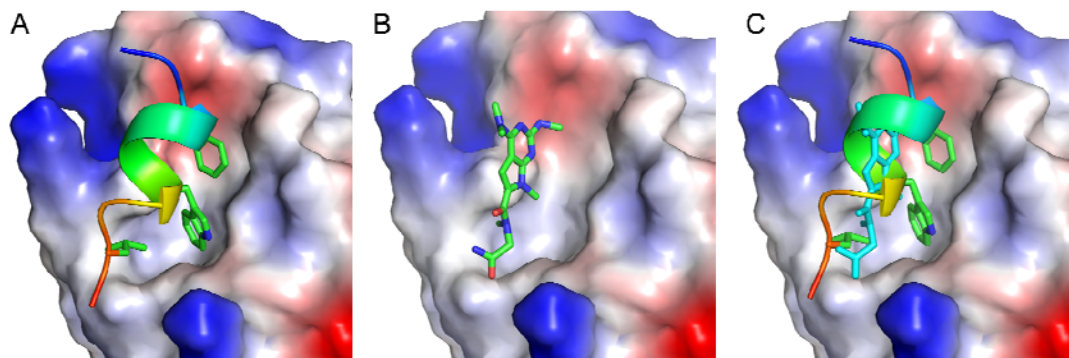


Figure S4. Fluorescence polarization (FP) assays to identify small-molecule inhibitors of the p53-MDMX and p53-MDM2 interaction. **(A)** A schematic representation of FP assays used to monitor the interactions between Rd-p53 peptide (SQETFSDLWKLLPEN-NH-Rhodamine) and MDMX or MDM2 protein. **(B)** The saturation curve of Rd-p53 peptide to recombinant MDMX¹⁻¹³⁷ and MDM2¹⁻¹³⁸ proteins. **(C)** Competitive binding curves of unlabeled p53 peptide (SQETFSDLWKLLPEN-NH₂) and MI-63 to the MDMX and MDM2 proteins. Each data point represents the mean and standard deviation of triplicate experiments. **(D)** Distribution of hits from the 900-compound library screen for MDMX inhibitors. Compounds above the 50% inhibition cutoff (red line) were selected as putative hits. The Z' factor score was 0.8.

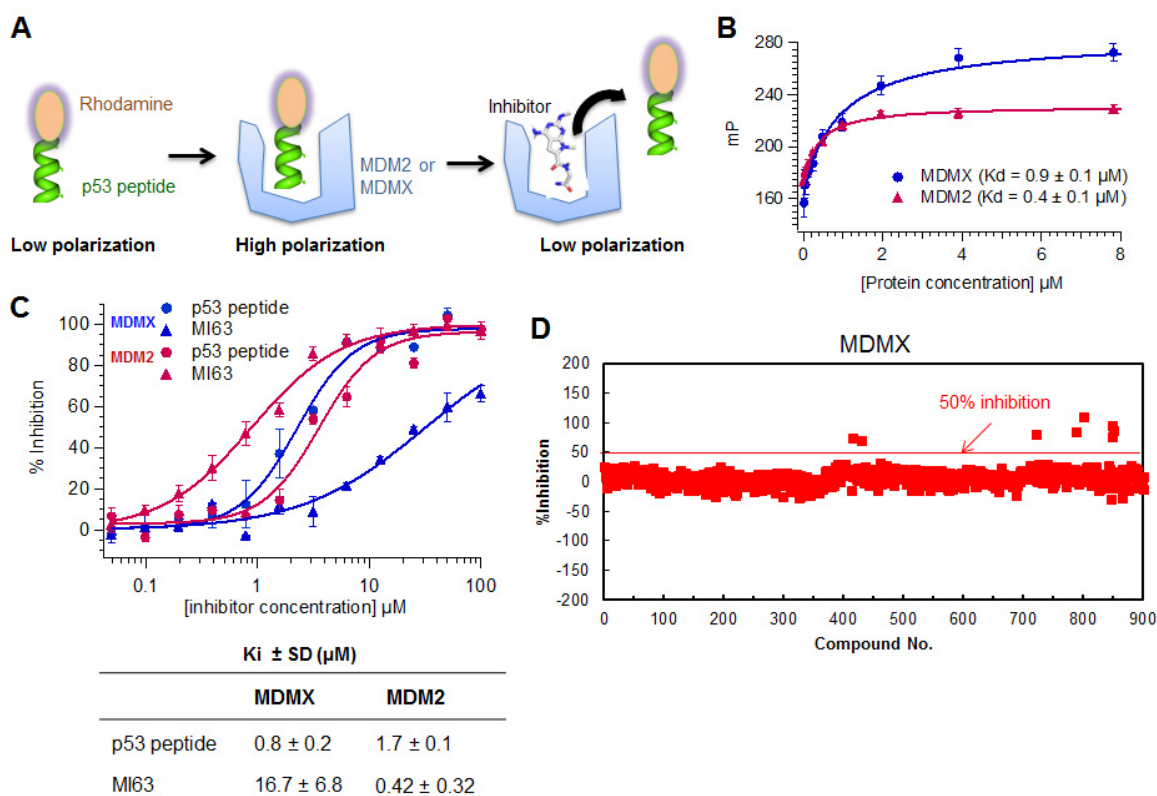


Figure S5. HPLC chromatograms and mass spectra of the purified **3a**, **3b** and NC-1.

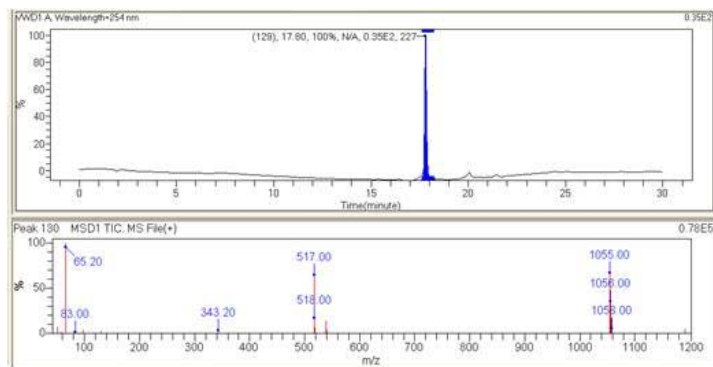
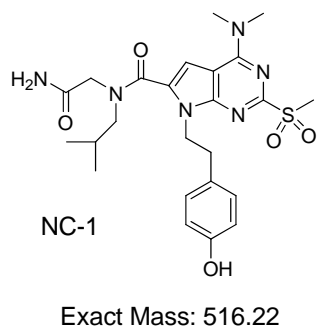
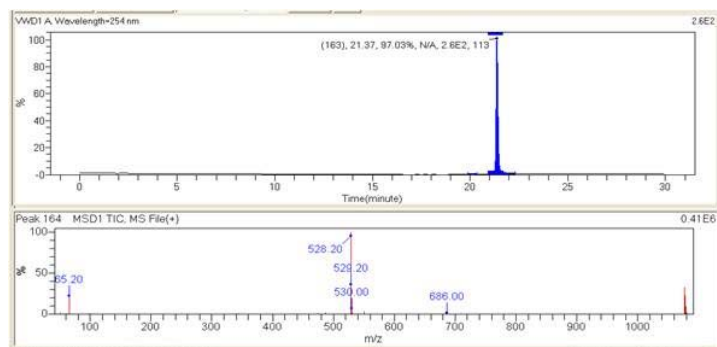
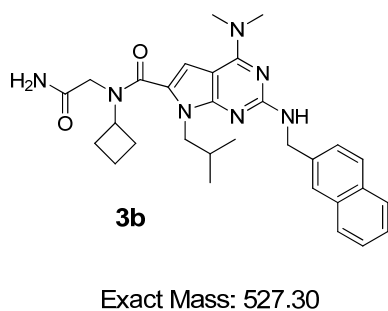
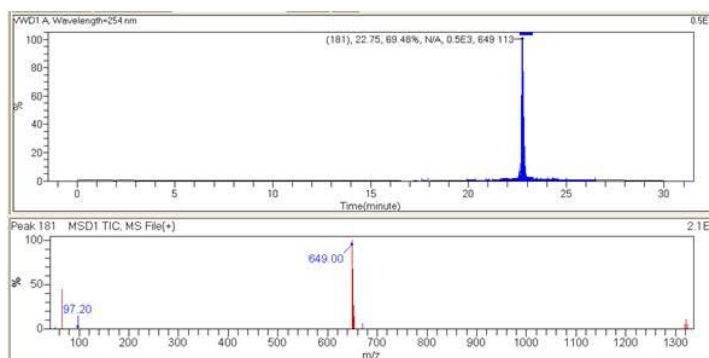
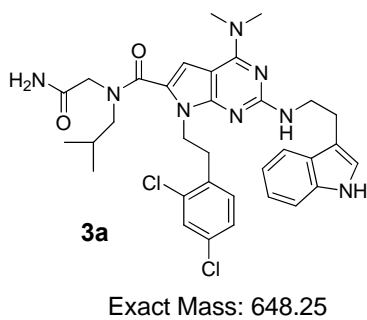


Figure S6. H460 cells were treated with DMSO, designated concentration of **3b** and 10 μ M NC-1 (a negative control) for 12 h and harvested for a Western blot analysis.

